# Correlation between Mount Wilson Classifications to Solar Flares using Solar Dynamics Observatory (SDO) and Hinode Satellites

*N.A.M. Norsham[1,2], Z.S. Hamidi[1,2*]*
*[1]Faculty of Applied Sciences, Universiti Teknologi MARA Shah Alam, 40450 Shah Alam, Selangor, Malaysia*
*[2]Institute of Science, Universiti Teknologi MARA Shah Alam, 40450 Shah Alam, Selangor, Malaysia*
**zetysh@uitm.edu.my*

*N.N.M. Shariff[2,3]*
*[3]Academy of Contemporary Islamic Studies (ACIS), Universiti Teknologi MARA Shah Alam, 40450 Shah Alam, Selangor, Malaysia*

ABSTRACT

*Space weather disruption is known to be caused by solar flares and coronal mass ejections, which is the motivation for this study. The Mount Wilson classification, or magnetic classification, is used to study sunspots or active regions (AR). Three active regions were analysed in this study to examine their correlation with flare production. We use statistical and observational analysis to identify our objective. Data used was from 2014 to 2019 and the associated ARs are AR 11967, AR 12403, and AR 12192. Further analysis was carried out on each of them using the white light, magnetogram, and AIA 1700 filter from Solar Dynamics Observatory (SDO,) NOAA (National Oceanic and Atmospheric Administration), Hinode, and Space Weather Live. According to this study, solar flares are associated with high magnetic flux density and the number and size of sunspots. There have been rearrangements and changes in the topology and energy of the magnetic field that resulted in a flare.*

**Keywords:** *Solar Flare; Coronal Mass Ejection; Mount Wilson Classification; Active Region*

ISSN 1823-5514, eISSN 2550-164X

Received for review: 2020-08-11
Accepted for publication: 2021-02-11
Published: 2022-01-15

## Introduction

The Sun, our star in the Solar System could eject a significant solar phenomenon that disrupts space weather. One phenomenon that is highlighted here is a solar flare. A solar flare is the enormous explosion of magnetic energy in the Sun and typically originates within the sunspot group. This is the site of magnetic reconnection and where the magnetic energy is released. When there is high energy radiation or particle acceleration from solar flares and coronal mass ejections (CMEs), another type of solar explosion, they can affect the satellites, global positioning system, and radio communication. This problem leads to the study of the solar flare as it can reach the Earth in a short time of only eight minutes. As solar flare production is related to the sunspot group, a scheme which is known as Mount Wilson is considered in this study.

Mount Wilson classification is a scheme used to categorize sunspots according to their magnetic properties and morphology. Many research studies used active regions' magnetics complexity to estimate their activities [1]-[3]. George Ellery Hale is the one that initiated this scheme in 1919 [4]. The idea of Mount Wilson is the usage of the magnetogram to classify magnetic polarities dispersion on the solar disk. At first, this scheme included only three designations of unipolar denoted by α, bipolar as β, and mixed polarity (γ). Later, a new configuration was added to the scheme and known as δ which means that a penumbra consists of two umbrae with opposite polarity as cited in [5]. Other than α, β and γ, there are some added designations of this scheme. There are i) δ, a qualifier to magnetic classes indicating that umbrae separated by less than 2 degrees within one penumbra have opposite polarity, ii) β- γ, a sunspot group that is bipolar, but which is sufficiently complex that no single, continuous line can be drawn between spots of opposite polarities, iii) β- δ, a sunspot group of general beta magnetic classification but containing one (or more) delta spot(s), iv) β- γ -δ, a sunspot group of beta-gamma magnetic classification but containing one (or more) delta spot(s).

From the Mount Wilson scheme explanation, this scheme is related to the sunspot group. Sunspot group or active region (AR) is associated with the production of solar flares and coronal mass ejections. Both events' output rates are varying between ARs [6]-[8]. A solar flare occurs as the stored magnetic energy in the solar atmosphere explodes from the Sun. This flare can be classified based on its brightness in X-ray wavelength. There are five categories of solar flares started with the intense to less intense flare which are X class flare, M, C, B, and A-class flare. In general, most of the sunspot is observed in alpha and beta configuration and bigger sunspot is usually linked to beta, beta-gamma, or beta-gamma-delta. The violent flare is commonly generated from the active region with delta designation as it consists of mixed magnetic polarity [9]. Besides, the powerful flare may occur in large, complex group sunspots that are linked to the delta spot's light bridges [10]. It is said

that sunspot size has a relation with the magnetic energy and magnetic field as both of them are proportional to each other, hence, as the size increases, so does the magnetic field and the energy [11]. Besides, the magnetic field of the Sun gets the energy from the rotating sunspots [12]. Thus, to calculate the maximum magnetic field strength at the umbra, a formula is picked for the calculation. The formula was formulated by [13]-[15] and is shown below in Equation (1).

$$B_m = \frac{3700\,A}{(A + 66)} \tag{1}$$

$B_m$ is a maximum magnetic flux density in the sunspot and A means the area of the spot. $B_m$ is calculated in unit Gauss (G) while A uses the millionths of the solar hemisphere (MH) unit. The magnetic field strength range is said to be 100 G (weakest) [16] and commonly around 3000 G (strongest). In complex sunspots, the strength of the bright area of light bridges can be 4300 G. Recently, the strongest field that was found is 6250 G [17].

The production of solar flares has been studied abundantly as this phenomenon could give an impact on space weather and the Earth. The emitted X-rays and ultraviolet radiation can cause long-duration radiation storms at Earth's ionosphere could destroy satellites and give harm to the spacecraft and astronauts.

## Methodology

The data of solar flares and its parameter were gathered from publicly available websites of NOAA (National Oceanic and Atmospheric Administration), Space Weather Live [18], Hinode and Helioviewer websites. NOAA website produces solar flare's soft X-ray data together with the duration of flare, location of active region, and classes of flare. The Hinode website from NASA provides XRT images of the Sun. The Helioviewer websites provide solar images from Solar Dynamic Observatory (SDO) satellites including magnetogram filters whereas the Space Weather Live platform gives access to magnetic classification of the sunspot. Table 1 shows the spacecraft specification of SDO and Hinode satellites. Since the satellite passes over the same spot on Earth at about the same time each day, downloading data is much easier. In less than an hour, the Sun's Energetic Particles cross 93 million miles to reach the Earth. The cause or source of these phenomena on the Sun remains unknown. Scientists have traced the origins of a solar energetic particle burst back to the Sun for the first time.

Table 1: Specification of Solar Dynamic Observatory (SDO) and Hinode satellites

| Satellite specification | Solar Dynamics Observatory (SDO) | Hinode |
|---|---|---|
| Manufacturer | Goddard Space Flight Center | JAXA / NASA / PPARC |
| Launch mass | 3,100 kg | 700 kg |
| Dry mass | 1,700 kg | 175 kg |
| Payload mass | 290 kg | 50 kg |

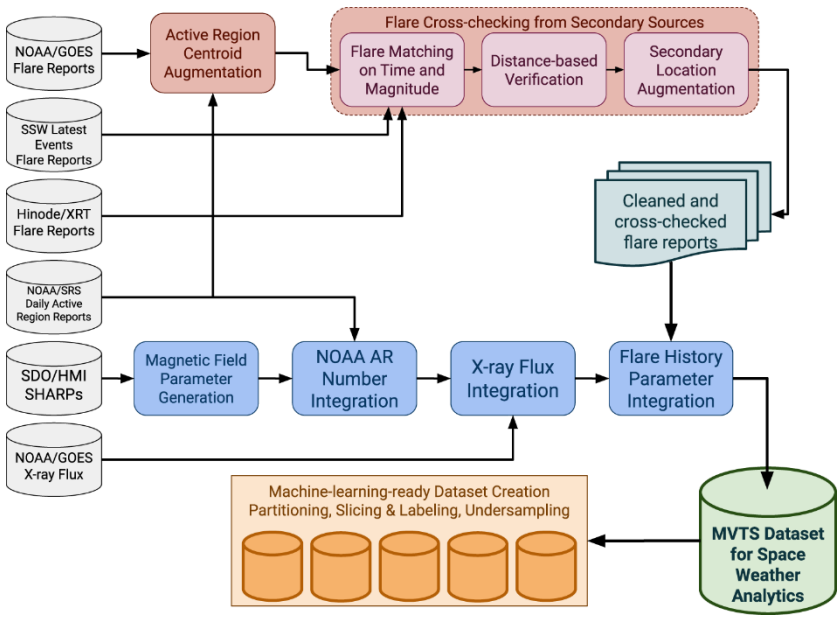


Figure 1: Schematic diagram of the solar flare and active regions processing data with the main parameters by different types of systems [19].

All these data then went through statistical analysis to see the relationship between magnetic classification and solar flare events. Then, the observational analysis was carried out by using the white light filter, magnetogram filter from SDO/HMI, and SDO/AIA of AIA 1700 that highlighted the site of intense concentration of magnetic fields lines. These filters help in studying the magnetic field of the sunspots or AR and associated solar flares. Typically, basic monthly reports include flare and sub flare data

as well as an individual day-by-day account of when the sun was photographed, monitored electronically, observed visually by different types of systems to cover the multi-wavelength range. There are several systems such as Solar H-alpha and White Light, magnetograms, Solar Dynamic Observatory (SDO), and Satellites including SOHO Solar Heliospheric Observatory and Hinode satellite to obtain all these data. Figure 1 shows the schematic diagram of the solar flare and active region processing data with the main parameters from different types of systems.

The Solar Dynamics Observatory (SDO) [20] system involves measurements of the Sun's interior and atmosphere, magnetic field, and energy output to better understand the Sun. SDO consists of EVE, HMI [21], and AIA [22] as presented in Figure 2. EVE stands for Extreme Ultraviolet Variability Experiment which measures the ultraviolet fluctuations from the Sun. HMI is the Helioseismic and Magnetic Imager that detects the Sun's magnetic field. While AIA is the Atmospheric Imaging Assembly comprised of 10 different wavelength bands to study the solar activity.

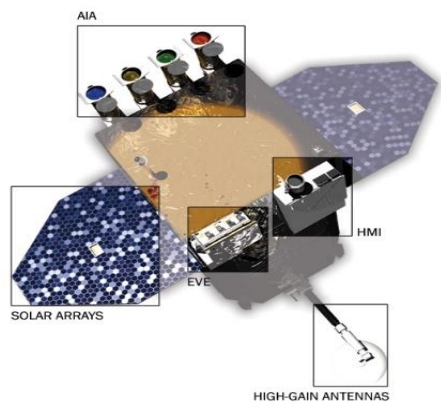


Figure 2: The SDO satellite [20].

Hinode [23], also known as Solar B, can measure the full vector magnetic field quantitatively on scales small enough to resolve elemental flux tubes. Due to its field of view and sensitivity, it can measure changes in the magnetic energy in both a steady-state (coronal heating) and a transient (flares, coronal mass ejections) manner in the solar atmosphere.

The Hinode satellite comprises the X-ray Telescope (XRT), the EUV Imaging Spectrometer (EIS), and the Solar Optical Telescope (SOT) [23]. The SOT includes the 50 cm aperture inside the Optical Telescope Assembly (OTA) and the camera system inside the Focal Plane Package (FPP) [24].

The electrical instrument configuration of SOT consists of Optical telescope Assembly (OTA), Tip-Tilt fold Mirror (CTM-TM), Polarization Modulation Unit (PMU), Focal Plane Package (FPP), main electronics box for FPP (FPP-E), power supply for FPP subsystem (FPPPWR), main electronics box for OTA and TTM (CTM-E), analogue driver for the TTM (CTM-TE), Mission Data Processor (MDP), spacecraft Data Handling Unit (DHU), and spacecraft central Data Recorder (DR) [25].

The other instrumentation of Hinode is XRT (X-Ray Telescope) that holds two optical systems, one for visible light and the other is for X-ray. Both visible and X-ray images are focused on a single CCD camera. Different filter images provide the temperature maps of the target object in the XRT field of view [26]. The EIS has spatially resolved spectra wavelength bands of 170 – 210 Å and 250- 290 Å. The telescope has a 1.9 m focal length and 150 mm mirror diameter with a total length of 3 m.

## Result and Discussion

In this section, solar flares data from 2014 until 2019 were statistically analysed to observe the connection between the flare classes and magnetic classes involved. Five magnetic classes are dominantly based on three different solar flare classes. We focused only on C, M, and X classes of solar flares since classes A and B are considered to be very minimum flare and occurred every day. Overall, there are 1805 events of a solar flare that occurred within six years. This magnetic class is important as an indicator of forecasting solar flares.

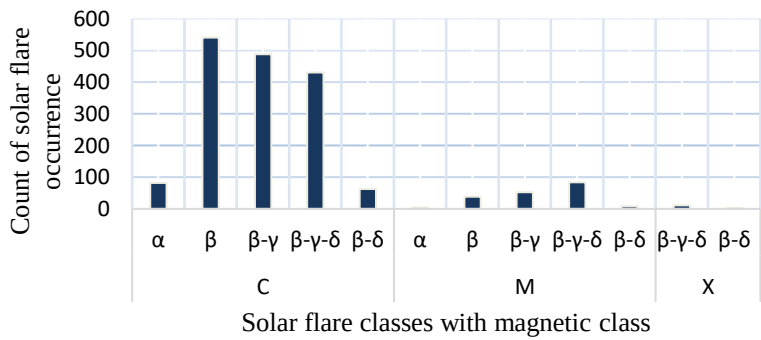


Figure 3: The count of magnetic class events related to solar flare classes of C, M, and X.

As displayed in Figure 3, the C class flare consists of the highest number of beta configurations and the least number of events for beta-delta configuration. For M and X flare classes, both shared the same highest configuration which is beta-gamma-delta with a low count of alpha and beta-delta designation of M and X classes respectively. Starting in 2014, the solar cycle experience a solar minimum with the decreasing number of sunspots produced. Thus, it is understandable if the production of large and intense flares has been decreased throughout the year from 2014 until 2019. Another statistical analysis had been performed to select the most significant active region (AR) related to the magnetic classification of the sunspot. The highest number of AR production was chosen as we believe they are categorized into important observations to be studied.

Table 2 showed available data obtained from each flare class. From the table, all three flare classes had the highest number of β- γ -δ spot occurrence compared to β and β-γ. In this case, we focused on only three active regions AR12403, AR11967, and AR12192 that represent each class of flare (C, M, and X). The structure of these sunspot shows a bipolar group that has more than one clear north-south polarity inversion line together with an umbra of opposite polarity together in a single penumbra. As mentioned before, a flare that occurred by the delta spot has the potential to produce a major solar flare. Then, detailed analysis for this AR was carried out in terms of the observation method where we used a magnetogram solar image filter to see the magnetic polarity of the selected region.

Table 2: Associated AR based on C, M, and X flare classes

| Flare Class | C | M | X |
|---|---|---|---|
| NOAA Number | AR 12403 | AR 11967 | AR 12192 |
| β | 4 | 2 | - |
| β-γ | 7 | - | - |
| β- γ -δ | 39 | 10 | 5 |

Interestingly, AR 12403 in C class flare produced three types of magnetic configuration which are β, β-γ, and β- γ -δ. Each spot count can be seen in Table 2 with β (4 counts), β-γ (7 counts), and β- γ -δ (39 counts) of flare events. In M class flare, AR 11967 formed two types of spots which are β and β- γ -δ with two flare and ten flare events respectively. For the X class of AR 12192, it only produced one type of magnetic configuration of β- γ -δ that consisted of five flare events. In this paper, we focus our analysis on the β- γ -δ spots as all flare classes contain this kind of configuration and are regarded as significant data to be analysed. So, for the first analysis, we went through AR 12403 details. Based on our data, this AR started its β- γ -δ spot on 23$^{rd}$ August 2015 until 28$^{th}$ August 2015. Then, we picked the flare event

on 26th August 2015 as it produced the highest flare intensity of C 9.5 and is relevant to be discussed for this paper. The magnetogram images of AR 12403 are shown in Figure 4.

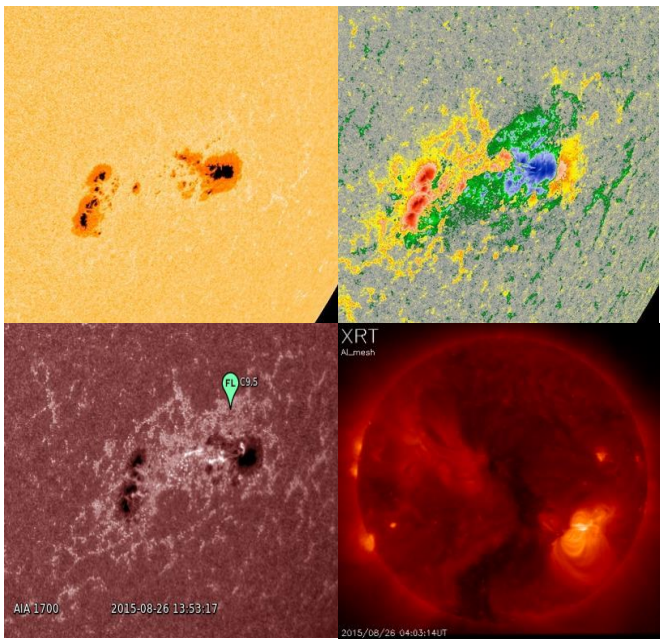


Figure 4: The Sun in the white light filter (top left) and magnetogram filter (top right), AIA 1700 wavelength (bottom left) and XRT filter (bottom right) of AR 12403 on 26th August 2015 (Source: SDO [20]/HMI [21]/AIA [22]/Hinode [23]).

Figure 4 represents the Sun images in magnetogram where they show the location and strength of the magnetic field of the Sun. In Figure 4, the top left plate is the active region on the Sun disk in a white light filter. The colourized the magnetogram (top right image), green and blue shows positive (South polarity) with blue indicating the strongest fields and red and yellow means negative (North polarity) with red of strongest fields. From the image of the magnetogram filter in the plate above, the leading spot is located on the West and the trailing spot on the Eastside. Based on the colourized magnetogram, the leading spot can be seen in blue representing the South polarity while the trailing spot in red indicated the North polarity.

As reflected in Figure 4 of colourized magnetogram, the blue and green area is more dominant with the bigger umbra size. Thus, there is laid the

strongest magnetic field of the sunspot and produced C 9.5 flare event. C9.5 peaked at 1353 UTC and it can be seen from Figure 4 (bottom image) in AIA 1700 band the site of the flare occurrence. The AR12403 spot size was 1190 and yielded 3506 G maximum magnetic flux although this AR showed signs of decay as the preceding and following sections of the group kept on distancing from each other and losing their magnetic complexity. The unstable magnetic configuration of this AR caused the changes in the magnetic field thus producing a high number of C class flares. This can be seen from the XRT filter as the magnetic field of AR12403 interact with each other. Another study on AR 12403 was conducted by [27] and concluded that β- γ -δ increased in the sunspot size which produces the C class flares.

For type M flare, the solar flare event on 30th January 2014 was selected. On this day, three M flares were detected produced from the same AR which are M6.6, M2.1, and M1.1. The focus on M 6.6 had the most intense flare that day.

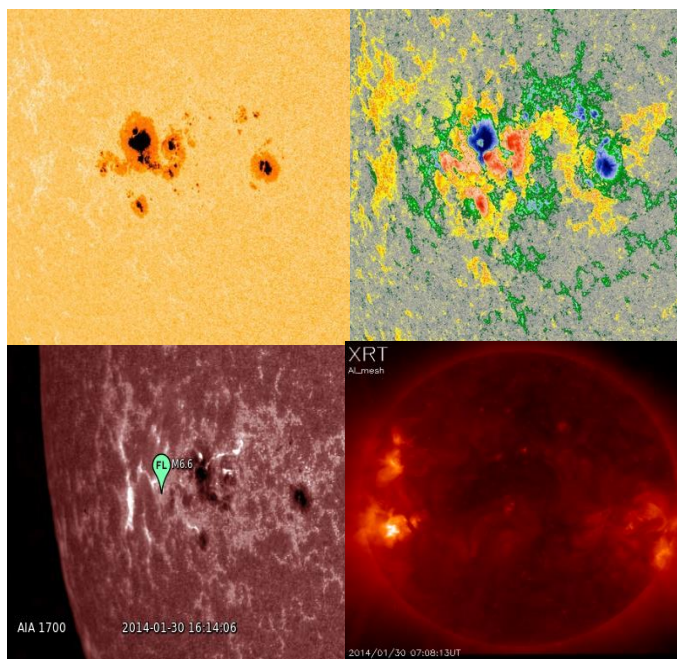


Figure 5: AR 11967 with M 6.6 flare on 30th January 2014. The top left is the Sun disk in white light, the top right shows the colourized magnetogram image and the bottom left image is the flare site seen in AIA 1700, and the Sun in the XRT filter band (Source: SDO [20]/AIA [22]/HMI [21]/Hinode [23]).

The strongest field for AR 11967 is the area of blue and red as shown in Figure 5, the top right image. It is a compact bipolar sunspot with North and South polarity in one region. The complex areas lead to the magnetic reconnection process as the flare exploded. This mechanism is one of the notable factors that help in improving our understanding of the Sun [28]. The M6.6 flare exploded at 1614 UTC. This AR has a spot size of 980 MH and 3467 G field strength. In the XRT band, the magnetic field produced a bright flare that caused it to produce multiple M class flares.

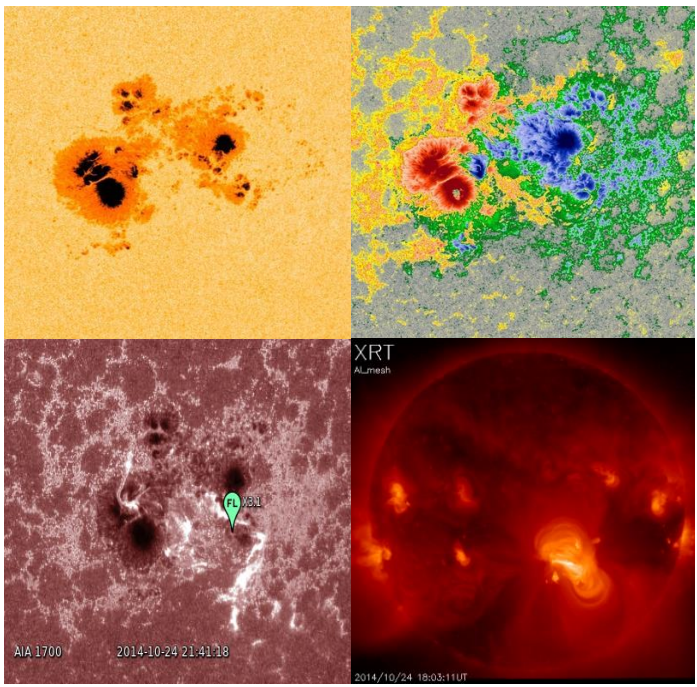


Figure 6: Sun images in the white light filter (top left), colourized magnetogram (top right) and AIA 1700 (bottom left) and XRT filter band of AR 12192 on 24th October 2014 (Source: SDO [20]/AIA [22]/HMI [20, 21]/Hinode[23]).

Figure 6 illustrates the structure of the sunspots using the magnetogram AIA1700 Angstrom. During this day, flares were produced in the red and blue areas due to the number of small sunspots and a strong magnetic field. The peak of Flare X3.1 occurred at 2141 UTC. In the AIA 1700 flare image, the pattern of the bright area highlighted the high magnetic field concentration. Besides, the production of the magnetic field by this AR can be observed by

the XRT image from Hinode as the large and bright flare appeared on the Sun's disk. The sunspot area of AR 12192 was 2740 MH and the maximum magnetic field was 3613 G. Accordingly, the evolution of the magnetic field has the potential to produce high solar activity with a long duration.

In all cases of solar flares related to AR mentioned in this study, the mechanism of occurrence was caused by the rearrangement of high conducting plasma in the magnetic topology. The rearrangement is usually related to the reconnection of the magnetic field [29-33]. This happens as the electrical resistivity of the plasma at the boundary layer against the required currents helps to maintain the changes in the magnetic field. Therefore, this triggers the magnetic energy to change into kinetic energy, particle acceleration, and thermal energy.

In previous studies by [7], the conclusion outline that β-γ-δ of AR is highly associated with the sunspot areas and the magnetic complexity. Based on this study, the β-γ-δ configuration of the AR produced a high number of solar flares in each C, M, and X class as compared to β and β-γ. This is thought to have relation to the size of the sunspots, magnetic strength, and number of sunspots.

## Conclusion

These three ARs (AR 11967, AR 12403, and AR 12192) went through a magnetic reconnection process hence, solar flares were produced at their respective peaked time. They are related to delta spot configuration and we believe this has to do with the active magnetic field as this is considered as the complex area with mixed magnetic polarities. The nearness of magnetic polarities to each other enables and causes high chances for a flare to explode. In addition, β- γ -δ has relation to sunspots size, magnetic strength, magnetic complexity, and a number of sunspots.

The size of sunspots seems to be related to the flares as the size increases, so does the maximum magnetic field strength. AR11967 had the least magnetic field strength while the strongest field was from AR12192 with a spot size of 2740. The size however related to the appearance number of sunspots on the Sun disk too. These three parameters depended on each other and cause the magnetic field energy to rise and thus, produced solar flares. After all, we can see and observe the magnetic field and activity of the Sun through the eye of the SDO and Hinode satellites hence enlightened us about the dynamical structure of the Sun.

## Acknowledgement

Heartfelt thanks goes to SDO/AIA/HMI, NOAA, Hinode, SWPC, Helioviewer, and Space Weather Live websites for providing their data accessible to the public. Helioviewer.org is part of the Helioviewer Project, an open-source project for the visualization of solar and heliospheric data. The Helioviewer Project is funded by ESA and NASA. The images on Helioviewer.org are credited to SDO (NASA), SOHO (ESA/NASA), STEREO (NASA), PROBA2 (ESA), Yohkoh (JAXA/NASA/PPARC), Hinode (JAXA/NASA/PPARC), GSFC, Royal Observatory of Belgium, LMSAL, SDAC, Stanford University, Harvard-Smithsonian Astrophysical Observatory, MSU/SDO-FFT. Hinode is a Japanese mission developed and launched by ISAS/JAXA, collaborating with NAOJ as a domestic partner, NASA and STFC (UK) as international partners. Scientific operation of the Hinode mission is conducted by the Hinode science team organized at ISAS/JAXA. This team mainly consists of scientists from institutes in the partner countries. Support for the post-launch operation is provided by JAXA and NAOJ(Japan), STFC (U.K.), NASA, ESA, and NSC (Norway). The authors also give full appreciation to the reviewers and editors for the beneficial comments and suggestions. This work was partially supported by the grant, 600-RMI/FRGS 5/3 (309/2019), YTR Grant 600-RMC/YTR/5/3 (001/2020), UiTM grants, and Kementerian Pengajian Tinggi Malaysia.

## References

[1] A. Cortie, "On the types of sun-spot disturbances," *The Astrophysical Journal,* vol. 13, pp. 260, 1901.
[2] P. S. McIntosh, "The classification of sunspot groups," *Solar Physics,* vol. 125, no. 2, pp. 251-267, 1990.
[3] K. R. Moon, V. Delouille, J. J. Li, R. De Visscher, F. Watson, and A. O. Hero, "Image patch analysis of sunspots and active regions-II. Clustering via matrix factorization," *Journal of Space Weather and Space Climate,* vol. 6, pp. A3, 2016.
[4] G. E. Hale, F. Ellerman, S. B. Nicholson, and A. H. Joy, "The magnetic polarity of sun-spots," *The Astrophysical Journal,* vol. 49, p. 153, 1919.
[5] S. Padinhatteeri, P. A. Higgins, D. S. Bloomfield, and P. T. Gallagher, "Automatic Detection of Magnetic $\delta $ in Sunspot Groups," *Solar Physics,* vol. 291, no. 1, pp. 41-53, 2016.
[6] I. Sammis, F. Tang, and H. Zirin, "The dependence of large flare occurrence on the magnetic structure of sunspots," *The Astrophysical Journal,* vol. 540, no. 1, pp. 583, 2000.

[7] K. Takizawa and R. Kitai, "Evolution and Flare Activity of $\delta $-Sunspots in Cycle 23," *Solar Physics,* vol. 290, no. 7, pp. 2093-2116, 2015.
[8] Z. Shi and J. Wang, "Delta-sunspots and X-class flares," *Solar physics,* vol. 149, no. 1, pp. 105-118, 1994.
[9] A. O. Benz, "Flare observations," *Living reviews in solar physics,* vol. 14, no. 1, pp. 2, 2017.
[10] W. Livingston, J. Harvey, O. Malanushenko, and L. Webster, "Sunspots with the strongest magnetic fields," *Solar Physics,* vol. 239, no. 1-2, pp. 41-68, 2006.
[11] S. Lin, D. Jinping, Z. Xiaoxin, and J. Yong, "Analysis of the Major Parameters in Solar Active Regions Based on the PCA Method," *Chinese Astronomy and Astrophysics,* vol. 39, no. 2, pp. 212-224, 2015.
[12] Z. Hamidi, M. Noh, W. Toni, and N. Shariff, "An Analysis of Active Region as a Trigger of Solar Flares," in *Journal of Physics: Conference Series*, vol. 1298, no. 1: IOP Publishing, pp. 012017, 2019.
[13] J. Houtgast and A. Van Sluiters, "Statistical investigations concerning the magnetic fields of sunspots I," *Bulletin of the Astronomical Institutes of the Netherlands,* vol. 10, pp. 325, 1948.
[14] S. B. Nicholson, "The area of a sun-spot and the intensity of its magnetic field," *Publications of the Astronomical Society of the Pacific,* vol. 45, pp. 51-53, 1933.
[15] T. S. Ringnes and E. Jensen, "On the relation between magnetic fields and areas of sunspots in the interval 1917-56," *Astrophysica Norvegica,* vol. 7, pp. 99, 1960.
[16] Y. Shi-Hui, *Magnetic fields of celestial Bodies*. Springer Science & Business Media, 2012.
[17] T. J. Okamoto and T. Sakurai, "Super-strong magnetic field in sunspots," *The Astrophysical Journal Letters,* vol. 852, no. 1, pp. L16, 2018.
[18] N. A. M. Norsham and Z. S. Hamidi, "A multiwavelength study of the Sunspot of active region which leads to X 17 solar flare," in *Journal of Physics: Conference Series*, vol. 1411, no. 1: IOP Publishing, pp. 012011, 2019.
[19] R. A. Angryk *et al.*, "Multivariate time series dataset for space weather data analytics," *Scientific data,* vol. 7, no. 1, pp. 1-13, 2020.
[20] W. D. Pesnell, B. J. Thompson, and P. Chamberlin, "The solar dynamics observatory (SDO)," in *The Solar Dynamics Observatory*: Springer, pp. 3-15, 2011.
[21] P. H. Scherrer *et al.*, "The helioseismic and magnetic imager (HMI) investigation for the solar dynamics observatory (SDO)," *Solar Physics,* vol. 275, no. 1, pp. 207-227, 2012.

[22] J. R. Lemen *et al.*, "The atmospheric imaging assembly (AIA) on the solar dynamics observatory (SDO)," in *The solar dynamics observatory*: Springer, pp. 17-40, 2011.
[23] T. Kosugi *et al.*, "The Hinode (Solar-B) mission: an overview," *The Hinode Mission*, pp. 5-19, 2007.
[24] K. Minesugi, T. Inoue, M. Tabata, T. Shimizu, T. Sakao, and Y. Katsukawa, "Telescope Co-Alignment Design and Its Performance On-Orbit of Solar Observational Satellite``Hinode"," *Transactions of the Japan Society for Aeronautical and Space Sciences*, vol. 56, no. 2, pp. 104-111, 2013.
[25] S. Tsuneta *et al.*, "The Solar Optical Telescope for the Hinode mission: an overview," *Solar Physics*, vol. 249, no. 2, pp. 167-196, 2008.
[26] T. Sakao *et al.*, "Focal plane CCD camera for the X-Ray Telescope (XRT) aboard SOLAR-B," in *Optical, Infrared, and Millimeter Space Telescopes*, vol. 5487: International Society for Optics and Photonics, pp. 1189-1198, 2004.
[27] S. Sabri *et al.*, "Geo-effective Disturbances from the “Beta-Gamma-Delta” Magnetic Fields on Active Region AR 2403," *World Scientific News*, vol. 37, pp. 1-11, 2016.
[28] Z. Hamidi *et al.*, "Magnetic Reconnection of Solar Flare Detected by Solar Radio Burst Type III," in *Journal of Physics: Conference Series*, vol. 539, no. 1: IOP Publishing, pp. 012006, 2014.
[29] K.-S. Cho, J. Lee, S.-C. Bong, Y.-H. Kim, B. Joshi, and Y.-D. Park, "A coronal mass ejection and hard X-ray emissions associated with the kink instability," *The Astrophysical Journal*, vol. 703, no. 1, pp. 1, 2009.
[30] P. Kumar, A. Srivastava, B. Filippov, and W. Uddin, "Multiwavelength study of the M8. 9/3B solar flare from AR NOAA 10960," *Solar Physics*, vol. 266, no. 1, pp. 39-58, 2010.
[31] A. Srivastava, T. Zaqarashvili, P. Kumar, and M. Khodachenko, "Observation of kink instability during small B5. 0 solar flare on 2007 June 4," *The Astrophysical Journal*, vol. 715, no. 1, pp. 292, 2010.
[32] C. Foullon, E. Verwichte, V. M. Nakariakov, K. Nykyri, and C. J. Farrugia, "Magnetic Kelvin-Helmholtz instability at the sun," *The Astrophysical Journal Letters*, vol. 729, no. 1, pp. L8, 2011.
[33] P. Kumar, A. K. Srivastava, B. Filippov, R. Erdélyi, and W. Uddin, "Multiwavelength observations of a failed flux rope in the eruption and associated M-class flare from NOAA AR 11045," *Solar Physics*, vol. 272, no. 2, pp. 301, 2011.